1

# Fuzzy Image Processing, Analysis and Visualization Methods for Hydro-Dams and Hydro-Sites Surveillance and Monitoring

Gordan Mihaela[1], Dancea Ovidiu[1], Cislariu Mihaela[1],
Stoian Ioan[2] and Vlaicu Aurel[1]
[1]*Technical University of Cluj-Napoca,*
[2]*S.C. IPA S.A. CIFATT Cluj,*
*Romania*

## 1. Introduction

The continuous surveillance, monitoring and operational planning of hydro-dams and hydro-sites is a very important issue, considering the impact of these critical structures on the environment, society, economy and ecology. On one hand, the failure of hydro-dams can dramatically affect the environment and humans; on the other hand, the operating policies must take into account the impact of the water resource exploitation on the hydro-site region and on the regions supplied by the reservoir.

The importance of periodic surveillance and monitoring through both objective measurements and subjective observations is emphasized by existing international standards, which provide the main surveillance and monitoring guidelines for hydro-dams and hydro-sites (CSED, 1983; DSC, 2010). Among other issues, these guidelines clearly state that the visual inspection of the hydro-dams and their surroundings is an important component of the surveillance process, as it aids the decision making process based on direct observations (CSED, 1983, pp. 21-28). Visual inspections complement the other type of data acquired from sensors and transducers placed within the dam body and its surroundings. It is a common practice in hydro-dam surveillance to store the visual observations by human observers in the form of visual observations records. Typically these records regard the state of the reservoir, banks and slopes, concrete structure and downstream valley, and are backed-up by digital image archives of the inspected structures (CSED, 1983; Bradlow *et al.*, 2002).

In respect to the water resource exploitation policy related to the hydro-sites, it is important to develop tools for water resource management evaluation and planning. However these should not be fully automated decision systems, but rather decision support components, to assist the human specialists in establishing the best operation policy. According to the EU Water Framework Directive (2000/60/EC), the water management plan must take into account the natural geographical and hydrological unit rather than the administrative or political boundaries (European Parliament, 2000). This assumes a thorough analysis of the

associated complex and heterogeneous data, to perform both the analysis of the current resource management policy and to predict the impact of some management policy on the environment, economy and society. Such a complex task is best performed by a computer decision support system, considering the amount and diversity of the required data/information to be processed. However since the decision on the best water resource management policy to be adopted is to be made by specialists, it is important to provide the decision support system with a human-compliant interface, both for introducing the input information and for displaying the assessment and prediction results in a meaningful and intuitive form to the end-user (this includes, besides numerical data, linguistic and qualitative assessments and, of course, a visual description of the results and recommendations, wherever this is possible). While adopting some existing fuzzy reasoning strategies for the evaluation of the water resource management policy, we mainly emphasize here on our contribution in the enhancement of the results presentation form – particularly on the visual presentation of the future effect of some particular policy, as a geo-typically textured map of the region, using image processing methods to transpose the numerical and qualitative assessment results into a suggestive visual representation.

Most of the solutions presented in this chapter were integrated in a hydro-dam and hydro-site surveillance system, devoted to the monitoring of the Tarnita hydro-site on the Somes River in Transilvania County, Romania. The details of the fuzzy image processing and analysis tools proposed are presented in the remaining of this chapter.

## 2. Problem formulation

Prior to the introduction of the proposed fuzzy image processing and analysis methods suitable to the visual examination of the concrete hydro-dams surface condition and to the visual rendering of the water resource management policy assessment in a hydro-site region, we consider necessary to give a description of the addressed problems. This should allow the reader to understand and acknowledge the fact that image processing methods may indeed play an important role in the assessment and evaluation of hydro-dams and hydro-sites, although this type of strategy is not so commonly encountered in the field. The following three subsections briefly point the roles of image processing and analysis methods, the role of artificial intelligence approaches and finally present the structure of the system we designed for hydro-dams/hydro-sites monitoring and surveillance, with an emphasize on the role of visual surveillance. Some of the significant references in the scientific literature related to the subject are also outlined.

### 2.1 The role of image processing and analysis methods in hydro-dams surveillance

In order to enhance the visual observations made by human experts, computer vision techniques may be employed. The approach is to acquire images and then, by the means of specific image processing algorithms, enhance and analyse them. Also, the periodical recording of these images into a database could prove very useful when monitoring the overall condition of the dam walls during time.

Less interest was oriented on incorporating image processing and analysis algorithms to automatically detect, diagnose and predict the behaviour of the dam and the possible faults

affecting the structure of the dam. The main interest in processing was to create a 3-D dam map, to be further investigated by the human operator, and even in this step, human intervention is often required. Taking into account the wide variety of computer vision algorithms currently available, is fair to consider that the automation of the visual inspection process of the dam, aiming to detect, diagnose and predict possible faults, can be further increased. Some of the methods presented in this chapter provide solutions to perform specific image processing and analysis tasks in the particular case of infrared and visible images of dam walls.

Bimodal analysis of optical and infrared images is a problem still needed to be tackled with. Few such applications have been reported, mainly in the fields of surveillance, people counting and tracking, robust skin detection (face detection), forest fires detection, or land mines detection (Ollero *et al.*, 1998; O'Conaire *et. al.*, 2006). However, for the diagnosis of dams such works are scarce, although infrared imaging is used extensively in assessing temperature loss, or poor isolations in buildings.

Thermal images can provide information about the scene being scanned which is not available from a visual image. Although much work has been performed for finding various image segmentation techniques in both imaging modalities, little efforts have been made for integration of complementary information extracted from the two imaging modalities.

### 2.2 The role of artificial intelligence techniques in hydro-sites operation monitoring

The significant development of the information systems puts nowadays its fingerprint on the hydro-sites surveillance and monitoring as well, with a strong emphasize on the design and implementation of intelligent systems to assist the specialists in the above mentioned areas. The artificial intelligence methods play a significant role in the development of systems devoted to dam surveillance and dam monitoring, especially in the form of decision support components and knowledge-based expert systems; among these methods, the well-known fuzzy theory and machine learning solutions (especially neural networks) are commonly employed. Some examples of such artificial intelligence based solutions for hydro-dams and hydro-sites surveillance, monitoring and assessments are briefly mentioned herein. Knowledge-based systems have been employed to assist the diagnosis of seepage from different types of hydro-dams (Asgian *et al.*, 1988; Sieh *et al.*, 1998). Neural networks are also employed in the investigation of seepage under concrete dams founded on rock (Ohnishi & Soliman, 1995) or in the estimation of the dam permeability (Najjar *et al.*, 1996). The joint use of fuzzy mathematics and neural networks is also reported by (Wen *et al.*, 2004), in the development of a bionics model of dam safety monitoring composed of integration control, inference engine, database, model base, graphics base, and input/output modules. Fuzzy logic and artificial neural networks were employed in the inference models building stage, needed to analyze and evaluate the run characteristics of dams.

### 2.3 Overview of the integrated hydro-site surveillance and monitoring system

Artificial intelligence techniques (including fuzzy logic, fuzzy knowledge based systems, neural networks and other supervised classifiers) have been extensively employed recently in hydro-dam and hydro-sites surveillance applications, as diagnostic tools and policy

recommendation tools. However, most existing solutions use measurements acquired from different sensors, and very few of them integrate visual observations obtained from some image analysis modules applied on digital images acquired during hydro-dams and hydro-sites monitoring. In this respect, we describe here a set of image analysis tools developed specifically for the concrete hydro-dams surveillance, which were implemented in the form of an integrated computer vision-based hydro-dam analysis system, capable of providing quantitative, qualitative and linguistic assessments of the concrete surface. The presented visual inspections and expert system components are part of a large hydro-dam and hydro-site surveillance system devoted to the monitoring of the Tarnita hydro-site on the Somes River in Transilvania County, Romania; its block diagram is illustrated in Fig. 1.

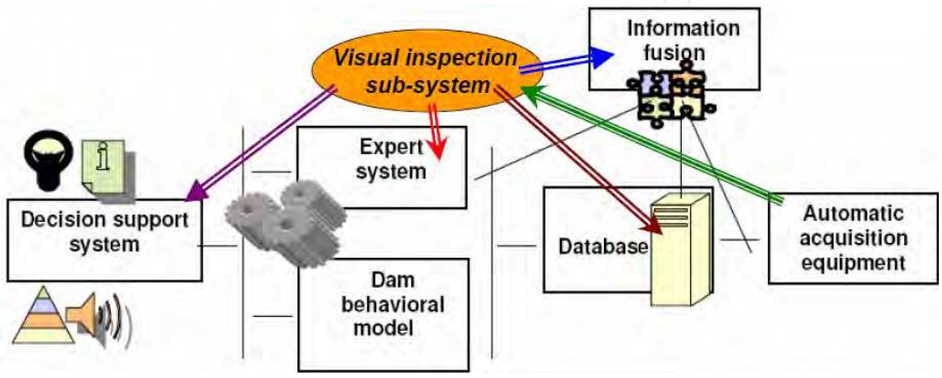


Fig. 1. The integrated system for dam safety decision support, using computer vision techniques and integrating the result of image analysis with the results of other data analysis modules

The automatic acquisition equipments collect multi-sensorial data from the sensors placed in the dam body. These equipments are: automatic acquisition station, capacitive sensor tele-pendulum, optical tele-pendulum, tele-limnimeter, laser telemeter, infrared and visible spectra cameras. All these data are stored into a relational multimodal database. The data fusion algorithms are used to extract relevant information regarding water infiltrations in the dam body, based on infrared and visible spectrum image fusion. Other image processing algorithms are applied to dam wall surface roughness examination, which is also likely to be caused by systematic water infiltrations. The dam models are used for dam behavior prediction and utilize the information stored in the database. The expert system use the human expert knowledge in specific domains and metadata resulted upon their own inference. The decision support system links the user with modeling components, image analysis and fusion modules, expert systems, and the database. Its role is to provide synthetic data in graphical, numerical and linguistic format, which would help the dam surveillance personnel in taking the right decisions regarding interventional measures that will prevent dam degradation and will ensure its functioning in good conditions. Another useful component that may be integrated in the system from Fig. 1 is the one devoted to water resource management policy evaluation and prediction in the hydro-site and the surrounding areas. Most commonly, such components are built using fuzzy rule base systems/fuzzy logic systems, as this mathematical framework is very suitable to handle both exact and approximate (qualitative or linguistic) knowledge, and this mixture of

information representation is often encountered in management evaluation systems. Our contribution in terms of a visually enhanced representation of the water resource management policy assessment results is also presented in the end of this chapter.

## 3. Downstream concrete surface evaluation of hydro-dams by image analysis

Visual inspection is a key element in dam monitoring process, allowing decisions to be made about dam behavior, based on direct observations. Visual inspections complement the data analysis process concerning different sensors and transducers placed within the dam body and it's surroundings, and the observations are filled in a standardized form describing the inspections results about: reservoir, banks and slopes, concrete structure, downstream valley. These records hold, for every feature observed, the procedures utilized during inspection as well as significant images illustrating the observations. Hence, once digital images of the inspected structure are available, a series of aspects are suitable for image analysis: detection and quantification of calcite deposits, detection of areas with humidity, evaluation of concrete surface of the wall in order to reveal structure faults or cracks, and so on.

It is a known fact that most cracks in dam walls have calcite exuding from them, indicating that moisture traversed the cracks (Abare, 2006). As water seeps through cracks, it leaves calcite deposits at the surface adjacent to the cracks. If the area between concrete layer is porous, the movement of water through them would accelerate the leaching action. Seepage samples may be collected, analyzed and compared to reservoir water to help determine whether soluble minerals pose a structural safety problem (Craft *et al*., 2007). Seepage could be estimated by estimating the volume of water required to precipitate the measured volumes of calcite in the unsaturated zone (Marshall *et al*., 2003). Besides these techniques, we will show that computer vision can also help detect and assess the calcite deposits and humidity of the concrete dam walls.

The deterioration of the concrete walls may also be an important concern as it may indicate the degradation of the downstream side, and to give an estimate of this type of degradation we proposed a solution to examine the surface roughness (Gordan *et al*., 2008). Besides an accurate identification of such deteriorations, we show that computer vision techniques help in providing a quantitative and qualitative description of the extent of the deterioration. It is important to note that all the results of the proposed computer vision techniques can easily be transcribed to the visual observation record and offer the advantage of an intuitive and natural presentation to the end user.

In terms of downstream concrete surface evaluation of dams, we propose the following:

1. A modified fuzzy c-means segmentation method (semi-supervised through the use of support vector regression) for the detection, localization and quantification of calcite areas in the plots of the downstream concrete surface of a hydro-dam. The difficulty of this image segmentation problem comes from the large variability of calcite deposits appearance, uneven distribution of data, variations of the concrete appearance depending on the acquisition conditions and devices. The proposed solution outperforms the classical segmentation algorithms in terms of accuracy (96% as compared to 91% with the classical fuzzy c-means).

2. Furthermore, since less severe infiltrations may only be visible in the infrared spectrum, we also propose an integration of infrared image analysis with the visible image analysis, using a late decision fusion to integrate the results of the two image analysis modules. The fusion is thought to take into account the spatial and temporal correlation of the two types of images of the same hydro-dam downstream surface. This approach should yield more reliable results in terms of infiltration assessment.

These algorithms and techniques are described in detail in the following sub-sections. The images to be processed are drawn from the multimodal database, which holds digital images of concrete dam walls. Such an image is illustrated in Fig. 2. These are cropped to elementary units, called sub-plots. Each sub-plot image is identified by information that allows later identification and association with the real scene (the identification data is: horizontal, vertical and plot number). Thus, it is easier to extract images from the same sub-plot taken at different dates or in different modalities (e.g. visible or infrared spectrum).

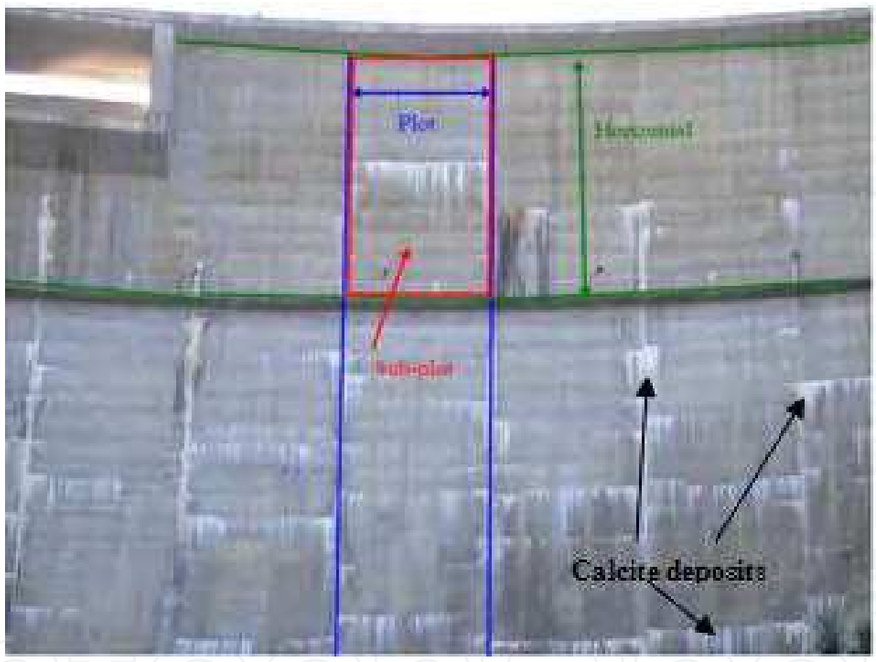


Fig. 2. Image sample at the input of the visual inspection module

### 3.1 Infiltration assessment by the analysis of calcite deposits using fuzzy segmentation

Calcite patches are good indicators of significant and time persistent water infiltrations; they are most likely to occur as being transported by the water infiltrations from concrete in the case of a repetitive water infiltration in a certain area of the dam. Therefore the problem of identifying the calcite formations on the concrete wall through an algorithm able to provide maximum accuracy despite the variability of appearance of calcite deposits, the variable lighting conditions on the portion of the wall, without knowing in advance if calcite is or is not present in the current image, or in what amount, must be tackled. These aspects make the calcite identification and assessment a rather difficult image analysis problem: the

significant variability of the calcite appearance makes almost impossible the derivation of a calcite appearance model to be used in the identification; model-free approaches seem more suitable, trying to identify natural pixels clusters, followed by an interpretation of the clustering results to identify if any represents calcite or not.

A rather powerful approach to non-supervised image segmentation by pixel clustering is the fuzzy c-means algorithm (FCM) (Dunn, 1973; Bezdek, 1981). Many variations of the FCM algorithm were successfully applied in image segmentation. Actually, various forms of fuzzy clustering have been employed to different image segmentation tasks. In (Chamorro *et al*., 2003), the segmentation of color images is achieved by a nested hierarchy of fuzzy partitions, based on a measure of color similarity. Starting from an initial fuzzy segmentation, a hierarchical approach, based on a similarity relation between regions, is employed to obtain a nested hierarchy of regions at different precision levels. Type 2 fuzzy sets are employed in (Clairet *et al*., 2006), for color images segmentation, to allow a better modeling of the uncertainty. A modified fuzzy c-means segmentation scheme with spatial constraints is introduced in (Hafiane *et al*., 2005), in the form of a two step segmentation method. Another fuzzy clustering method, with no constraints on the number of clusters, aiming to segment an image in homogeneous regions, is presented in (Das *et al*., 2006).

The solution that we proposed for the segmentation of the calcite deposits on the concrete hydro-dam walls images is more application-targeted (and it worth noting that it may be also generalized to other application-specific segmentation tasks, as it provides a framework to incorporate a-priori knowledge in the fuzzy c-means cost function). Details on this approach may also be found in (Dancea *et al*., 2010). The calcite identification on the concrete dam wall can be treated as a pixel classification problem. As there is no prior knowledge regarding the shape of the calcite deposits, the spatial constraints are not really helpful in the segmentation; the colors of the pixels are the only relevant features to consider. An important fact to consider however is the amount of the calcite deposits on each dam wall image, which is significantly smaller than the entire wall region. If we build a data set to be clustered comprising all the pixels in the currently analyzed image, classified into calcite and non-calcite samples, this set will be highly unbalanced among the classes of interest, and this is an unfavorable situation in a classification task, being prone to more errors in the poor represented class. This situation can be partially overcame by defining the classification data as the set of distinct colors in the concrete dam wall image, each color being included only once. From the several possible color spaces, we prefer the natural Red Green Blue (RGB) representation, as it is just as suitable as others for Euclidian distance based classifiers; thus each sample (corresponding to a color from the image) is represented by a vector $\mathbf{x} = \begin{bmatrix} R & G & B \end{bmatrix}^T$. The image to be segmented is considered to be a sub-plot image of a dam wall, as shown in Fig. 2. Therefore the current data set is formed by the colors in this sub-plot color image, $X_C = \left\{ \mathbf{x}_i \middle| i = 1,2,...,N_C \right\}$, where $N_C$ denotes the number of distinct colors in the current image. Our goal is to classify/cluster the data in $X_C$ in one of two possible classes of interest: calcite deposit – denoted by $C_C$, and not calcite – denoted here by $\overline{C}_C$. Although this is actually nothing else but a binary classification problem, trying to solve it by an unsupervised fuzzy c-means clustering of the data in only two classes will risk to be unable to group all the colors corresponding to the class "anything else

but calcite", since their variance is too large. Therefore a larger number of classes than two only will be needed in the initial clustering, one per dominant color. An examination of the sub-plots shows that generally two dominant colors are present in the non-calcite sub-plot areas: a grayish like color corresponding to the concrete and a brown-black color corresponding to organic deposits. Thus a 3-class clustering should be performed, with two classes for the $\overline{C}_C$ dataset and one the calcite, $C_C$.

The fuzzy c-means algorithm (Bezdek, 1981) is a very efficient clustering procedure when the number of clusters is known a-priori, aiming to find natural fuzzy groupings of the data according to their similarity in respect to a selected distance metric. In the end of an iterative objective function minimization process, the optimal class centers and membership degrees of the data to be clustered are found, with the optimality defined as the minimization of the classification uncertainty among the data in the classes. However a good clustering result is only achieved if the amount of data in each cluster is relatively balanced; otherwise the expected fuzzy centroid of the class with fewest data can be rather different than the real centroid of the class. This is mainly due to the fact that although the distance between the data and the resulting class center is large (leading to a large cost in the objective function), if the number of these terms is negligible in comparison to the size of the data set, it will contribute insignificantly to the total cost. While we already tried to avoid this case by taking all the colors in the sub-plot only once, this caution might still not be enough to guarantee a balanced data set. Therefore, furthermore, we propose to apply a modified objective function in the fuzzy c-means clustering, which assigns a higher penalty to the misclassification of the expected calcite pixels colors, that is, of the lighter colors in the data set $X_C$. We should mention here that, although the number of pixels colors corresponding to the organic deposits (brown-black, that means – dark-most) is also much smaller than of the grayish pixels, we are not concerned about their misclassification here, as in the worse case, the color of a brown-dark pixel is closer to a grayish pixel than to a calcite one, and then the misclassified data for the organic deposits can never appear in the calcite class $C_C$.

Let us denote by C – the number of classes to which the $N_C$ samples x from the set $X_C$ are to be assigned in some membership degree; in our case, C=3. The membership degrees of the data to the classes is stored in a matrix $U\left[C \times N_C\right]$, where the $u_{ji}$ element, j=1,...,C and i=1,...,$N_C$, represents the membership degree of the vector $\mathbf{x}_i$ to the class j. Each line in U is the discrete representation of the fuzzy set corresponding to a data class. The C fuzzy sets are constrained to form a fuzzy partition of the data set $X_C$. Starting from any initial fuzzy partition of the data set to be fuzzy classified $X_C$, the algorithm aims to optimize the partition in the sense of minimizing the uncertainty regarding the membership of every data $x_i$, i=1,…,$N_C$, to each of the classes. In the proposed weighted fuzzy c-means algorithm, we introduce a set of class-specific scalar positive weights $w_j$, j=1,…,C, to assign different relative importance to the distances of the data in $X_C$ to each of the classes centers. With these weights, we build a fuzzy c-means weighted objective function in the form:

$$J_{w,m}(U,V) = \sum_{i=1}^{N_C} \sum_{j=1}^{C} u_{ji}^{m} \cdot w_j \cdot d^2\left(\mathbf{x}_i, \mathbf{v}_j\right) \tag{1}$$

whose minimization is done iteratively, as in the standard fuzzy c-means algorithm, using the following equations for the computation of the fuzzy class centers $v_j$ and for the fuzzy membership degrees $u_{ji}$:

$$\mathbf{v}_j = \frac{\sum_{i=1}^{N_C} u_{ji}\mathbf{x}_i}{\sum_{i=1}^{N_C} u_{ji}};\ u_{ji} = \left( \sum_{l=1}^{C} \left( \frac{w_j \cdot d\left(\mathbf{x}_i, \mathbf{v}_j\right)^2}{w_l \cdot d\left(\mathbf{x}_i, \mathbf{v}_l\right)^2} \right)^{\frac{1}{m-1}} \right)^{-1} \tag{2}$$

In the expressions above, V is the set of the class centers, $V=\{v_1,..,v_C\}$, $v_j \in \Re^3$; m is a parameter controlling the shape of the resulting clusters (typically m=2); $d(\cdot,\cdot)$ is a distance norm in the RGB space between any two vectors. A common choice for d, used in our approach as well, is the Euclidian distance. The iterative process ends when the change in either U or V is under a certain tolerance (error) (in theory, arbitrarily small).

The three weights $w_1$, $w_2$ and $w_3$ are estimated roughly using the shape of the histogram of the brightness component of the segmented image; the shape descriptor which proves useful for our case is the skew of the histogram, as it provides a numerical measure of the distribution of the samples to the left and right of their mean. Using solely the brightness and not the color is sufficient for our goal, as our concern is to be able to "differentiate" the light-most class (which accounts for calcite as explained above) from the other two classes. Therefore we give default fixed weights to the non-calcite classes and tune just the calcite class weight as indicated by the histogram's skew. Considering an N sample set formed by the brightness values of the pixels in the currently analyzed sub-plot, $\{y_1, y_2, ..., y_N\}$, the sample's skew $\gamma$ can be estimated as the ratio between the third central moment of the sample and the cube of the sample's standard deviation:

$$\gamma = \frac{\mu_3}{\mu_2^{\frac{3}{2}}} = \frac{\frac{1}{N}\sum_{i=1}^{N}\left(y_i - \bar{y}\right)^3}{\left(\frac{1}{N}\sum_{i=1}^{N}\left(y_i - \bar{y}\right)^2\right)^{\frac{3}{2}}},\ \bar{y} = \frac{1}{N}\sum_{i=1}^{N} y_i. \tag{3}$$

For a uni-modal histogram having the gray levels are evenly distributed around the mode, the skew is close to zero. If more darker pixels than brighter pixels are present in the examined image, the skew $\gamma$ will be negative. On the opposite, if the brighter pixels are dominant and outnumber the darker ones, $\gamma$ will be positive. Based on these considerations, we can perform the following adjustment of the calcite class weight depending on the skew $\gamma$ (assuming the other two classes have fixed weights). If $\gamma$ is positive (i.e., the number of light pixels accounted for calcite is large enough), there is no need to enhance the importance of the calcite class in respect to the other two, and we can set the calcite weight equal to the other classes. If $\gamma$ is negative or near zero, it indicates the areas of calcite are rather small as compared to the examined surface, so the calcite class weight should be increased. Intuitively, the more negative $\gamma$ is, the larger the weight assigned to the calcite class should be.

Note that although there is no a-priori association of the class index j, j=1,2 or 3, and the brightness of the colors in the class, we always know that the fuzzy class with light most colors is the fuzzy class whose center is the lightest, and this class will be considered to correspond to the calcite (if any):

$$C_C = C_k \left| k = \underset{j=1,2,3}{\operatorname{argmax}} \left( \left[ 0.299 \quad 0.587 \quad 0.114 \right] \cdot \mathbf{v}_j \right). \right. \tag{4}$$

To be able to effectively employ the above considerations into our algorithm, a numerical mapping between the range of values γ and the range of weights of the light-most, i.e. calcite pixels class, must be obtained. Denoting our target weight by $w_k$, with k given by Eq. (4), we search for the mapping $w_k(\gamma)$ that best fits a set of training data, obtained by manually tuning the value $w_k$ on a set of statistically significant dam wall images (with enough variability in appearance, to cover as many practical cases as possible). A set of 15 images of several sub-plots, with different aspect, under different lighting conditions and different amounts of calcite (from none to very severe) have been selected and manually analyzed to optimize the calcite class' weight for an accurate calcite identification. The pairs formed by the skew values and the best manually selected weight values $w_k$ have been collected, and an interpolation procedure based on support vector regression (SVR) has been applied on this training set to completely define in an automatic fashion the computation of the weight $w_k$. We assumed the other two classes' weights "fixed" to 1.

The reason for using SVR in the interpolation step is its proven good performance when only a relatively sparse set of data points is available. Based on Vapnik and Chervonenkis's statistical learning theory (Vapnik, 1998), support vector learning principle allows handling successfully difficult cases, with better precision and recall than other learning methods. This is mainly due to the structural risk minimization principle implemented by SVMs. SVMs were initially "built" for classification and later extended to the regression issue – SVR – by introducing a loss function (Scholkoph *et al.*, 1998; Platt, 2000). Starting from an input data set, represented by a vector x, the SVM learns the functional dependency between input and output, represented in the form of a scalar-valued function f(x). The expression of the regression function provided as a result of learning by an SVM is:

$$f(\mathbf{x}) = \sum_{i=1}^{L} \left( \alpha_i - \alpha_i^* \right) K(\mathbf{x}, \mathbf{x}_i), \tag{5}$$

where L denotes the total number of training data, $\alpha_i$ and $\alpha^*_i$ are their associated Lagrange multipliers, and the function $K(x,x_i)$ represents a kernel function used for mapping the input data in a higher dimensional input space. In our experiments, a polynomial kernel of degree 7 was considered. According to the observed skew values in our images, its range was limited to [-2;2]. The range of values for the weights $w_k$ is chosen to be [1;10]. The resulting mapping $w_k(\gamma)$, after applying SVR on the training set is represented in Fig. 3.

Experiments were run on a set of 15 large, high resolution images, from which we chose 60 manually segmented sub-plots (as illustrated in Fig.2). The performance of the proposed segmentation method was assessed on the test set of 60 sub-plots, using a previously manually drawn ground truth (on which the calcite regions were manually marked). The

difference between the ground truth segmentation and the segmentation result of our algorithm allows us to assess the segmentation error, the false positives and the false negatives for the calcite class. The segmentation error for the calcite class achieved with our method, expressed as the average percentage of misclassified pixels in the test set for the total 60 sub-plots, is 4.19%, whereas for the standard fuzzy c-means algorithm is 9.64%(more than double). Some segmentation results are illustrated in Fig. 4.

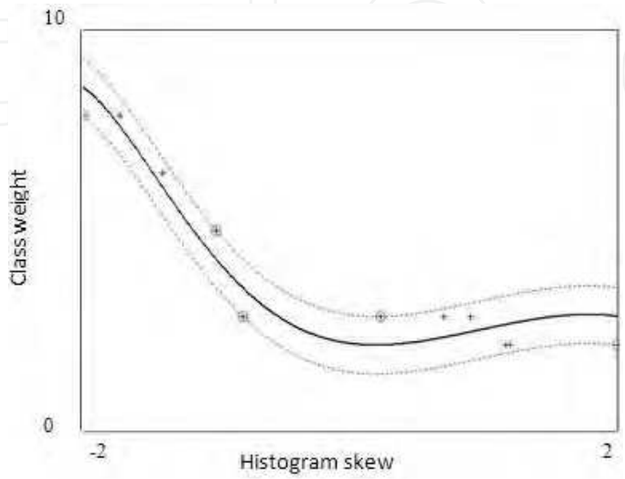


Fig. 3. Skew to class weight mapping

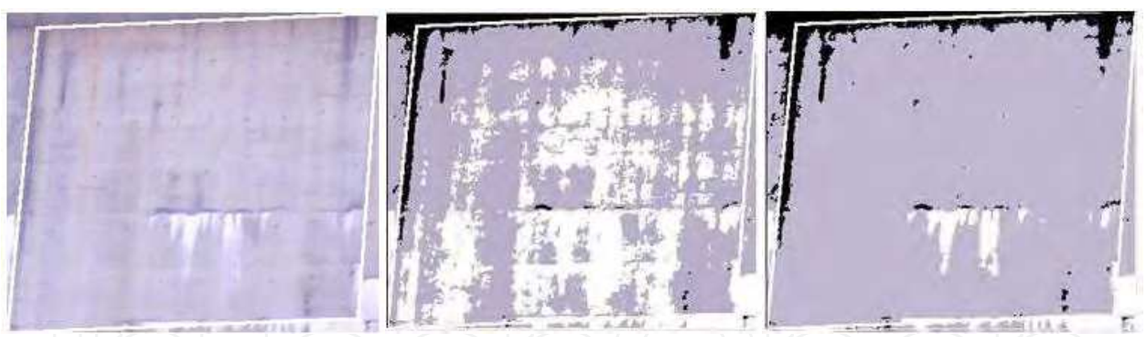

(a) (b) (c)

Fig. 4. Example of the calcite segmentation for a sub-plot: (a) the original (not segmented) sub-plot image; (b) the fuzzy c-means segmentation result; (c) the proposed weighted fuzzy c-means segmentation result.

Despite the good performance of this segmentation procedure in the localization of calcite, one must take into account that less severe infiltrations may not produce significant calcite deposits yet, and may only be visible in the infrared spectrum. Therefore the integration of infrared image analysis results with the visible image analysis results, using a late decision fusion, can bring more valuable information in the infiltration assessment. The fusion is thought to take into account the spatial and temporal correlation of the two types of images of the same hydro-dam downstream surface. This approach is presented in the following sub-section.

### 3.2 Bimodal infiltration assessment through the integration of infrared and visible information

The block diagram of the bimodal fusion based approach for water infiltration assessment is schematically illustrated in Figure 5. Many of the operations involved in the acquisition and low level processing of the visible spectrum and infrared spectrum images are done independently (in a parallel processing fashion). Apart from the acquisition, these operations include: visible spectrum and infrared spectrum images delimitation at plot level (as shown in Figure 2); visible and infrared image segmentation and infiltration severity degree mapping in the two imaging modalities for the quantitative description of water infiltration information. On the output of the corresponding stages, we simultaneously have the two water infiltration degrees maps decided by the two modalities, to integrate these decisions by a simple fusion process.

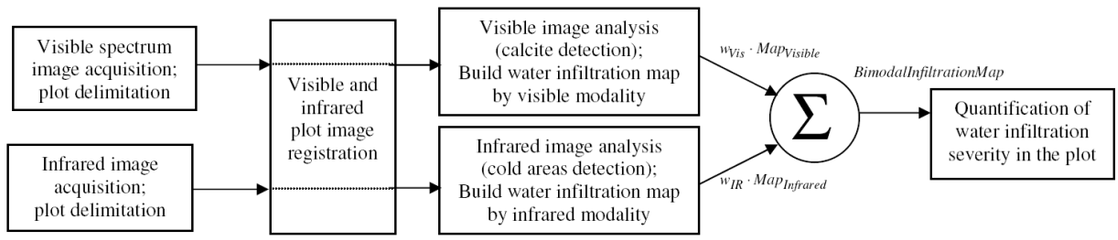


Fig. 5. Block diagram of the proposed method for infiltration assessment within the dam body

After the acquisition step, a registered pair of sub-plot images is available to be taken from the visual inspections database, each corresponding to the same element. The processing described in the following refers to such an aligned pair. For the infrared image acquisition we used a thermal camera with temperature coding capabilities (providing a thermal map of the corresponding dam wall area). We refer the image of the currently analysed plot in the visible spectrum as "the visible image" and the image of the same plot in the infrared domain will be referred as "the infrared image" and we assumed they are pixel-level registered by scaling and translation compensation. An example of such a registered (visible, infrared) image pair for a plot of the dam wall is shown in Figure 6.

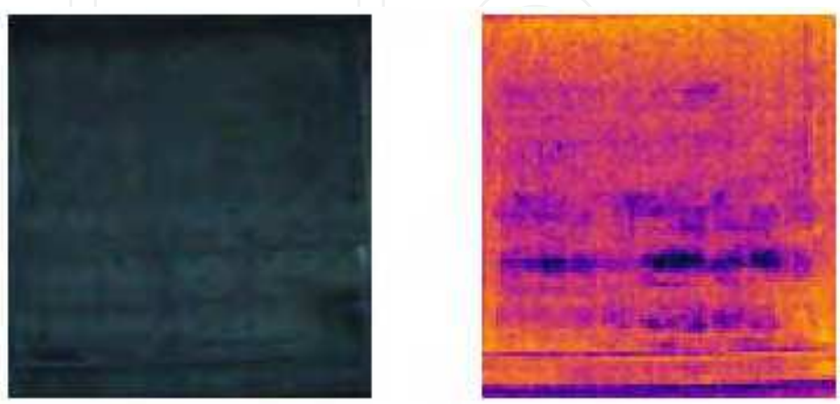

Fig. 6. A pair of images for a hydro-dam wall plot acquired in the two modalities: visible spectrum modality (left) and infrared modality (right)

The visible image analysis and segmentation for calcite detection was already presented in the previous sub-section. For the bi-modal analysis we discuss here, a further step is required: the creation of the ”water infiltration map” in the visible domain. This map must actually illustrate the severity of the water infiltration, but this severity is (as discussed priorly) correlated to the ”amount” or severity of the calcite deposits: in the areas where the water infiltrated on a long period of time, the calcite deposits will appear brighter, as the calcite layer is thicker. We map the severity degree of water infiltration to an intensity range {0,1,...,255}, with 0 for the lack of any infiltration to 255 for maximum severity infiltration. Accordingly we can convert the segmented ”visible image” (with calcite areas identified as explained in the previous sub-section) into a visible infiltration severity degree map. To do so, we consider that the brightness component Y is a sufficiently good indicator of the "whiteness" of the calcite – therefore, of the severity of the infiltration also. We represent in matrix form the brightness component of the ”visible image” from the current plot pair by $I_Y[H\times W]$, with elements in the range {0,1,...,255}. Let us consider the segmented plot image, with the pixels assigned to one of the two classes: calcite or non-calcite, represented as a binary matrix as well, $S_{Vis}[H\times W]$. With these notations we build the water infiltration map of the visible image as the matrix $Map_{Visible}[H\times W]$, according to the following expression:

$$\mathrm{Map}_{\mathrm{Visible}} = \frac{\mathbf{S}_{\mathrm{Vis}}(i,j)\cdot \mathbf{I}_{\mathrm{Y}}(i,j)\cdot 255}{\mathrm{Y}_{\mathrm{Max,Calcite}}} \tag{6}$$

where $Y_{Max,Calcite}$ is the maximum possible intensity for calcite areas, derived from a set of training images corresponding to calcite patches on the hydro-dam wall. An example of a water infiltration map for the „visible image” in the left side of Figure 6 is illustrated in Figure 7.

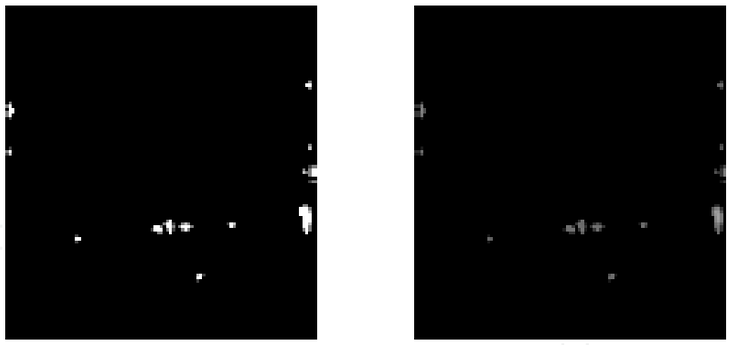

Fig. 7. Plot image segmentation result in the visible domain: Calcite against not calcite segmented image (left) and infiltration severity degree map (right)

On the other hand, the infrared image analysis and segmentation aims to identify the cold areas, to produce a water infiltration map from the infrared image of the plot. It is known that, at least in the spring/summer, when the ambient temperature is rather high, the areas of the plot with water infiltrations appear colder in the plot’s thermal map. The more significant the water infiltration is, the colder is the local part of the plot, thus the lower the temperature on the plot’s thermal map. However we can expect that in such areas little evidence of calcite will be identified in the visible image, since the calcite is likely to occur in

the region below the wet areas. This gives reason to believe that the two information sources can favourably complement each other. Since in the case of the thermal maps we always have available exactly the color-temperature conversion scale, we can use this scale and a-priori knowledge about the numerical range related to the qualifier „cold" to obtain the accurate identification of the water infiltration areas. An example of the selected scale portion, as considered to represent water infiltrations in our application (the severity of the infiltrations is stronger as the color is closer to violet and dark violet than to red), is illustrated in Figure 8. The red color is considered to be already not cold at all, whereas the very dark violet is considered to be the coldest possible. The simplest way to convert this color scale into a scalar scale in the range {0,1,...,255}, with 0 for the minimum coldness and 255 for the maximum coldness, is to use the negative of the red color component intensity of the scale image, as shown in Figure 8.

Fig. 8. The cold temperature part of the infrared scale: Original (left); its red component (right)

The segmentation process of the infrared image of the plot into cold areas and not cold areas is done pixel wise, based on the pixel color. The RGB space is uniformly quantized with only 4 bits per color component to guarantee the color match of the "infrared image" pixels with the infrared scale. We also gather and denote by SCold the set of the quantized color intensities in the RGB representation of the IR scale corresponding to cold from Figure 8, and simply assign the pixels in the infrared image of the plot the label 1 if their quantized color is found in SCold, and 0 otherwise. As a result, we obtain the segmented infrared image of the plot into cold against not cold areas, described by the matrix $S_{IR}$ [H×W].

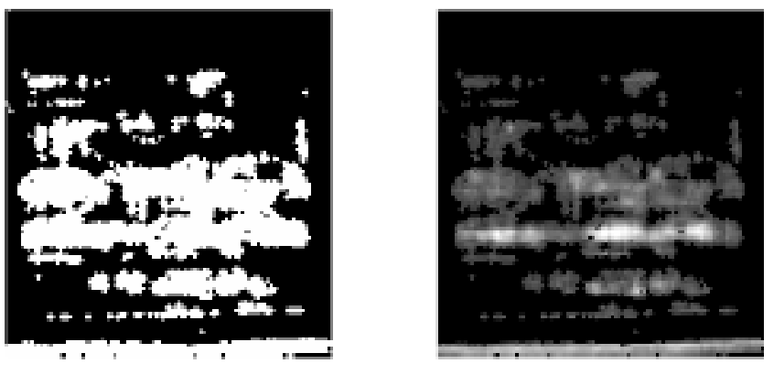

Fig. 9. Plot image segmentation result in the infrared domain: Cold against not cold segmented image (left) and infiltration severity degree map (right)

Afterwards, we build the water infiltration severity degree map in the infrared domain – similar to the one in the visible domain. However in the infrared case, we consider as infiltration severity degree indicator – the negative of the red color component in each pixel position previously classified as cold, as discussed earlier. Let us denote by $Map_{Infrared}$[H×W] – the severity degree map of the water infiltration in the infrared modality, represented in the range {0,1,...,255}. The values in this matrix are computed as:

$$Map_{Infrared}(i,j) = S_{IR}(i,j) \cdot \left(255 - I_{R,IR}(i,j)\right) \quad (7)$$

where $I_{R,IR}[H \times W]$ represents the intensity of the red component in the infrared image of the current plot.

The segmentation result in "cold" and "not cold" areas for the infrared plot image given in Figure 6, where the segmented image is presented as a binary image (black – "not cold", white – "cold"), and its associated water infiltration severity degree map, are given in Fig. 9.

The final processing step is the bimodal fusion of visible and infrared water infiltration severity information. We use the two individual information sources already provided by the independent image processing and analysis stages: the visible and infrared image processing, to obtain the overall assessment and quantification of the water infiltration amount in the currently analysed plot. Several fusion schemes are available, varying from very simple (pixel-based) to complex ones, to perform the information integration from two or more modalities; the most used in particular for visible and infrared bimodal information fusion can be found in (Yin and Malcolm, 2000; O'Conaire *et al*., 2006). Among these, one of the simplest schemes is by weighted averaging of the decisions given by each modality alone at pixel level, provided that the visible and infrared image registration was previously performed. Let us denote the decision about the plausibility of presence of a certain event in the spatial position (i,j) in the visible spectrum modality by $d_{Vis}(i,j)$ and the decision about the plausibility of presence of the same event in the spatial position (i,j) in the infrared modality by $d_{IR}(i,j)$. We also consider the weights (confidences) assigned to each modality denoted by $w_{Vis}$ and $w_{IR}$, chosen to satisfy the constraints: $w_{Vis} \in (0;1)$; $w_{IR} \in (0;1)$; $w_{Vis} + w_{IR} = 1$. The confidences $w_{Vis}$ and $w_{IR}$ assigned to each modality are derived based on expert's knowledge about the relative significance of each modality in assessing the severity of the water infiltration. The presence of calcite shows persistant, longer duration water infiltration in the plot, thus its weight should be higher than the infrared's information source weight. We chose as confidence values in our application: $w_{Vis}$=0.65 and $w_{IR}$=0.35. As information sources to be weighted aggregated, we use the individual water infiltration severity degrees maps, $Map_{Vis}$ and $Map_{IR}$. The overall water infiltration severity degree map, represented as an intensity image in the range {0,1,⋯,255}, with 255 – maximum infiltration severity, is obtained as:

$$InfMap(i,j) = w_{Vis} \cdot Map_{Vis}(i,j) + w_{IR} \cdot Map_{IR}(i,j). \quad (8)$$

An example of the resulting water infiltration severity degree map after bimodal image fusion, for the plot presented in Fig. 6, is given in Fig. 10. Then this overall decision map can be used to compute quantitative descriptors of the water infiltration amount and local severity on the plot. Examples of such simple quantitative descriptors are given in (Gordan *et al*., 2007): the percentage of the water infiltration area from the total plot area; the maximum local severity degree of water infiltration, assessed as the accumulated severity of the infiltration reported to the total area exhibiting infiltration.

In order to test this method we used the same multi-modal database containing images acquired from Tarnita dam, near Cluj-Napoca. We selected 5 pairs of plots acquired in both

modalities (visible and infrared). As shown earlier in this section, a ground truth for visible image segmentation into calcite areas and non-calcite areas can be easily obtained, and the same – a ground truth for pixel classification into cold areas for the infrared images. Thus we can assess the functionality of these processing stages very accurately. However, this is not the case for the assessment of water infiltrations severity, which in general can only be subjectively estimated by human observers. Therefore we can only roughly compare the results provided by our algorithm, converted to subjective scales, to subjective (human) evaluation of the water infiltrations based on the visible and infrared plot image evaluation. These comparative results for the 5 pairs of plots are presented in Table 1. The only difference from the human expert's opinion is in the 4th line in Table 1, for a plot exhibiting water infiltration in a very small area, in respect to the local severity of the water infiltration: although the numerical results show a large local value, the human expert identifies it as not significant, and this could be explained by the overall assessment done by the human expert, with almost no attention to local details when the water infiltration region size is not significant. The segmentation results, both for the visible and infrared plot images show in all cases good accuracy.

Although we employ here one of the most simple fusion schemes, we can see how the use of the two modalities can lead to better results than the analysis of each imaging modality alone. Also, the implementation of the joint analysis of visible and infrared images into the visual inspections module we described at the beginning of this chapter, has the advantage of providing numerical estimates of the extension of the water infiltrations and severity of the water infiltrations in the plots, reducing the risk of human observer subjectivity and image display quality.

| Plot pair Number | Water Infiltration Area | Infiltration Severity | Infiltration amount (subjective) | Infiltration severity (subjective) |
|---|---|---|---|---|
| 1 | 32.05% | 81% | Medium/Large | Severe |
| 2 | 23.63% | 58% | Medium | Moderate |
| 3 | 24.46% | 64.7% | Medium/Small | Moderate |
| 4 | 2.4% | 72% | Almost none | Reduced |
| 5 | 43.7% | 78% | Large | Severe |

Table 1. Quantitative results of our algorithm against subjective human expert's opinion

## 4. Assessment of the water resources management policy in a hydro-site region

As the hydro-dams reservoirs are also the main water supply resources for the geographical region, the assessment of the water management policy in the operation of the hydro-dam in respect to various economical and environmental factors is also an issue of significant interest. In this respect, we propose and implement a fuzzy decision support component to help in assessing the water resource management. Whereas the evaluation strategy itself is inspired by the work of (Zhou & Huang, 2007), employing a hierarchical process analysis strategy with qualitative reasoning, the presentation of the assessment results is novel, as we aim to display the evaluation not only in numerical and linguistic form, but also in a visual

form. The originality of the presented solution consists in the presentation of the water resource management evaluation "grading" in the form of a geotypical textured map of the region, where the natural texture changes according to the evaluation result for a specific category and according to the qualifier assigned to the management policy (varying from worst to very good). Therefore, in this sub-section we primarily emphasize on this visualization enhanced results presentation part. The interested reader may find more details of the implementation of the tool in (Gordan *et al*., 2010).

To achieve a meaningful graphical representation, we propose to employ fuzzy alpha-blending, image morphology and fuzzy image inpainting algorithms, which allow the production of high quality and meaningful geotypically textured maps of the hydro-site region. This allows the user to get multiple clues on the results of the water resource management evaluation, and have a stronger impact than the numerical assessment alone. The advancements and new application tracks of image processing algorithms and display devices provide the means for advanced graphical representations to be easily integrated in decision support software tools. These components are not so widely employed in the existing systems, but some implementations exist, as e.g. the integrated information management and simulation system combining WebGIS, database and hydrological model in (Shaomin *et al*., 2009) – which integrates a flood simulator and visually presents the flooded areas; or, the GIS based integrated system, which also incorporates hydrological analysis and cascade hydroelectric station dispatching functions, with powerful visualization tools (Shi *et al*., 2006).

The case of water resource management assessment may significantly benefit from a visualization module provided in the form of a geotypically textured map of the evaluated region. This can easily embed digital maps and natural images specific to the site, combined with specifically designed rendering tools. The fuzzy evaluation process results should drive the rendering of the appropriate textures on the digital map of the region.

Adopting the terminology in (Zhou & Huang, 2007), the factors involved in the assessment of the water resource management are called indexes. Each index represents a relevant attribute in the water resource management evaluation, and it must allow either a numerical or a qualitative description. During the system's setup, a weight must be assigned to each index, showing its relevance in the assessment of the water resource management. The weights may vary depending on the available water resources in the region and on the overall regional conditions. As the water resource management may impact several facets of life (the natural resources of the region, the ecology and the environment, the society and the economy of the region), a group of indexes is defined for each category individually. This will allow an independent evaluation of the water resource management policy's impact on each category. So far we implemented the decision support component only for the category of natural resources. This implies the definition of the appropriate set of relevant indexes for the natural resources, influenced by the water management policy.

As shown in the literature, five indexes are most relevant for the natural resources category in the framework of water resource management: the total water resources; the water resources per capita; the utilization rate of the water resources; the annual rainfall; the water shortage rate (Zhou & Huang, 2007). These five indexes are grouped into the index layer of the component. Based on their current values and on the management evaluation procedure, the

quality of the water resource management policy in respect to the natural resources preservation is expressed in terms of five fuzzy qualifiers: Worst, Bad, Moderate, Good and Best, grouped in the output layer of the component – known as the "condition layer".

The decision support component for the evaluation of water resource management policy in respect to the natural resources preservation must include a so-called training phase, in which the specialist helps defining the fuzzy sets membership functions associated to each index and each linguistic qualifier in a set Q={*Worst*, *Bad*, *Moderate*, *Good*, *Best*} (in respect to the specific category), and the weights of the indexes in the evaluation. Then, in the evaluation phase, the current values of the indexes – let us consider them given in the form of a vector x - are provided to the input of the system. Based on the values in x, the evaluation algorithm computes a membership degrees vector u[1×5], showing the confidence in assigning the currently examined water management policy to the fuzzy categories from Q, in the *Worst* to *Best* order. The vector u of confidence degrees in the suitability of each linguistic qualifier for the current water management policy in respect to the resource category is also used in the visual rendering sub-system.

The visual rendering of the evaluation results is achieved as follows. Assume that, for the current geographical region, we have its geographical map, with some manual marking of the interest categories, as e.g. the one shown in Figure 10, for the Somes river basin in Romania, corresponding to a good operation situation. Starting from this image, we would like to generate two geotypically textured images: one corresponding to the *Worst* resource management case, in which the exploitation was not proper, and one corresponding to the *Best* resource management case, with a very good water resource management policy.

In principle, the *Best* case geotypically textured map simply needs some texture synthesis applied on the image in Figure 10, using suitable natural textures for the forest, water, rock – and the approach we employed to generate the natural looking textured map was a modified version of the exemplar-based image inpainting approach of (Criminisi *et al*., 2003). An example of inpainting the forest region over the map from Figure 10 is shown in Figure 11. However, in the *Worst* case image, it would be good to also apply some additional processing; a suitable choice is to perform some morphological operations – as: erosion of the rivers; dilation of the mountain area, to enhance the visual effect of a very bad policy, prior to inpainting the map with the suitable textures.

Once the two geotypically textured images corresponding to the two extreme water resource management qualifiers are created, we would like to display any intermediate results as given by our assessment fuzzy system. Consider the two images represented as three-dimensional matrices $I_{Worst}$ and $I_{Best}$, of size $W_I \times H_I \times 3$ each, where $W_I$ is the image width, $H_I$ - the image height, and 3 is the number of color components per image. We already have available the degrees in which the management of the water resources can be considered *Worst* (the value of the first component from the vector u), *Bad* (the value of the second component from u), *Moderate* (the value of the third component from u), *Good* (the value of the fourth component from u) and *Best* (the value of the last component from u). The only thing to be done is to combine the two images $I_{Worst}$ and $I_{Best}$ to obtain the correct visualization as a new image $I_{Result}$, according to:

$$I_{Result} = \alpha \cdot I_{Best} + (1 - \alpha) \cdot I_{Worst}, \tag{9}$$

where α is some blending factor ranging between 0 and 1, generated at the output of a Takagi-Sugeno fuzzy system, with the following configuration:

1. Input fuzzy sets: the five linguistic qualifiers (*Worst*, *Bad*, *Moderate*, *Good*, *Best*)
2. Output fuzzy sets: five singletons – one for each reference value α, corresponding to the reference case of a *Worst*, *Bad*, *Moderate*, *Good* or *Best* management. These values were chosen intuitively and empirically to: $A_{Worst}=A_1=0$; $A_{Bad}=A_2=0.2$; $A_{Moderate}=A_3=0.5$; $A_{Good}=A_4=0.8$; $A_{Best}=A_5=1$
3. Rule base: five fuzzy rules, associating each qualifier to an output singleton, in the form: $R_k$: If *Qualifier* is $q$ then $\alpha=A_k$, $k=1,2,...,5$; $q$ = { *Worst*, *Bad*, *Moderate*, *Good*, *Best*}.

As the result of the Takagi-Sugeno inference, the output value for the blending factor $\alpha$ is given by: $\alpha = \dfrac{\sum_{k=1}^{5} u_k \cdot A_k}{\sum_{k=1}^{5} u_k}$.

The results of the assessment are illustrated for two different cases of indexes' values: close to best management and between bad and moderate, but not worst management, as shown in Figure 12. The results are compliant to the observer's expectations.

Fig. 10. Illustration of the Somes River Basin marked map, to be further processed in visualization purposes


Fig. 11. Illustration of an inpainting result for the forest region with a natural texture, corresponding to the best resource management case

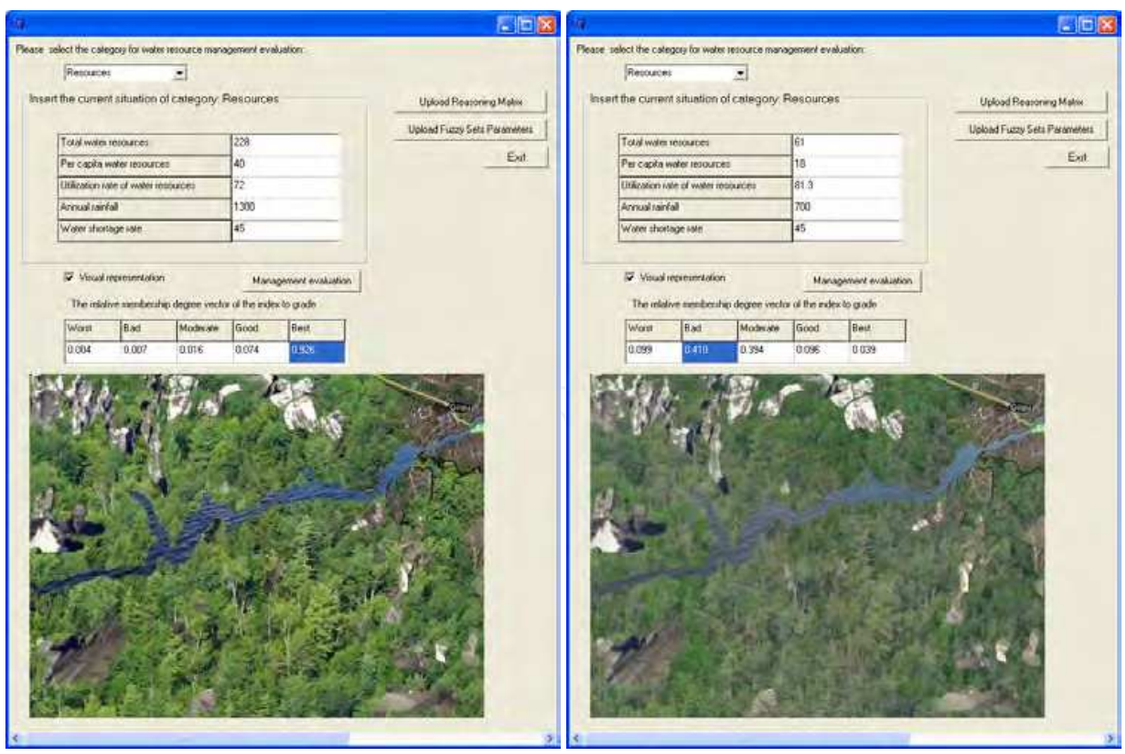


Fig. 12. Illustration of the water resource management policy assessment for the *Resource* category for: The *Best* management case (confidence 0.926) (left); The *Bad* to *Moderate* management case (confidence 0.41 for *Bad* and 0.39 to *Moderate*) (right)

## 5. Conclusion

This chapter aimed to present a series of novel fuzzy image processing methods and algorithms implemented in the rather general framework of hydro-dams and hydro-sites surveillance, monitoring and assessments, emphasizing on their theoretical motivation and results. Most of these methods have been employed in a hydro-dam and hydro-site integrated system for the safety decision support of these critical structures, thus the results are verified on real image data. Future work still needs to be done in this field, as the integration of the presented fuzzy image analysis algorithms (especially for the visible and infrared modalities) is just in its beginning; other imaging modalities as e.g. sonar, as well as the underwater examination of the hydro-dam structure would be of significant interest. Furthermore, the integration of the hydro-sites surveillance systems with water resource management policy assessment in the region operated by the dam reservoirs is another challenging issue.

## 6. Acknowledgment

Part of the work described in this chapter, as well as the implementation of the system in Romania and the image acquisition, was performed with the support of the project no. 705/2006 in the frame of CEEX research and development programme, financed by Romanian Government

## 7. References

Abare, R. (2006). Shotcrete done right. Failed repair teaches lessons about shotcrete. *Public Works Magazine*, January 1, Retrieved from http://goliath.ecnext.com/coms2/gi_0199-5268853/Shotcrete-done-right-failed-repair.html

Asgian, M.I., Arulmoli, K., Miller, W.O., and Sanjeevan, K. (1988). An expert system for diagnosis and treatment of dam seepage problems, In: *Microcomputer knowledge-based expert systems in Civil Engineering*, Adeli, H., pp. 118-126, American Society of Civil Engineers (ASCE), ISBN 9780872626539, New York, N.Y.

Bezdek, J. C. (1981). *Pattern Recognition with Fuzzy Objective Function Algorithms,* Plenum Press, ISBN 0306406713, New York, N.Y.

Bradlow, D., Palmieri, A., and Salman, S. (2002). *Regulatory Frameworks for Dam Safety: A Comparative Study*, World Bank Publications, ISBN 0821351915, Washington, D.C.

Chamorro-Martinez, J., Sanchez, D., Prados-Suarez, B., Galan-Perales, E., and Vila, M.A. (2003). A hierarchical approach to fuzzy segmentation of colour images, *Proceedings of the 12th IEEE International Conference on Fuzzy Systems,* Vol. 2, pp. 966 – 971, ISBN 0-7803-7810-5, St. Louis, MO, May 2003

Clairet, J., Bigand, A., and Colot, O. (2006). Color Image Segmentation using Type-2 Fuzzy Sets, *Proceedings of the 1st IEEE International Conference on E-Learning in Industrial Electronics*, pp. 52 – 57, ISBN 1-4244-0324-3, Hammamet, Tunisia, December 2006

National Research Council (U.S.) Committee on the Safety of Existing Dams (CSED) (1983). *Safety of existing dams: evaluation and improvement*, National Academy Press, ISBN 030903387X, Washington, D.C.

Craft, C.D., Pearson, R.M., and Hurcomb, D. (2007). Mineral Dissolution and Dam Seepage Chemistry – The Bureau of Reclamation Experience, *Proceedings of the 2007 National Meeting, Dam Safety 2007*, Austin Texas, Lexington, Retrieved from http://www.craftgeochemistry.com/CraftMineralDissolutionASDSOmeeting2007.pdf

Criminisi, A., Pérez, P., and Toyama, K. (2003). Object Removal by Exemplar-Based Inpainting, *Proceedings of the IEEE Computer Society Conference on Computer Vision and Pattern Recognition (CVPR) 2003,* Vol. 2, No. 2, pp.721-728, ISBN 0769519008, Madison, WI, June 2003

Dam Safety Committee (DSC) (2010). *Surveillance Reports for Dams*, Retrieved from http://www.damsafety.nsw.gov.au/DSC/Download/Info_Sheets_PDF/General/DSC2C.pdf

Dancea, O., Tsatos, O., Gordan, M., and Vlaicu, A. (2010). Adaptive fuzzy c-means through support vector regression for segmentation of calcite deposits on concrete dam walls, *Proceedings of the 2010 IEEE International Conference on Automation, Quality and Testing, Robotics (AQTR 2010)*, Vol. 3, pp. 293-298, ISBN 978-1-4244-6724-2, Cluj-Napoca, Romania, May 2010

Das, S., Konar, A., and Chakraborty, U.K. (2006). Automatic Fuzzy Segmentation of Images with Differential Evolution, *Proceedings of the IEEE Congress on Evolutionary Computation (CEC 2006),* pp. 2026 – 2033, ISBN 0-7803-9487-9, Vancouver, BC, Canada, July 2006

Dunn, J. C. (1973). A Fuzzy Relative of the ISODATA Process and Its Use in Detecting Compact Well-Separated Clusters. *Journal of Cybernetics*, Vol. 3, No. 3, pp. 32-57, ISSN 0022-0280

European Parliament (2000). Directive 2000/60/EC (The EU Water Framework Directive). *Official Journal of the European Communities*, Vol. OJ L 327, pp. 1-72, ISSN 1725-2423

Gordan, M., Dancea, O., Vlaicu, A., Stoian, I., Tsatos, O., and Oltean, G. (2007). Hydro-dams Security Assessment by Visible and Infrared Image Fusion, *Proceedings of the 1st IFAC Workshop on Convergence of Information Technologies and Control Methods with Power Plants and Power Systems (ICPS'07)*, pp. 234-239, ISBN 978-973-713-180-5, Cluj-Napoca, Romania, July 2007

Gordan, M., Dancea, O., Vlaicu, A., Stoian, I., and Tsatos, O. (2008). Computer Vision Support Tool for Assessing Concrete Hydro-Dams Surface Deterioration. *Journal of Control Engineering and Applied Informatics*, Vol. 10, No. 2, pp. 68-75, ISSN 1454-8658

Gordan, M., Florea, C., Dancea, O., Stancel, E., and Tsatos, O. (2010). A visualization enhanced fuzzy decision support tool for water resource management tasks, *Proceedings of the 2010 IEEE International Conference on Automation, Quality and Testing, Robotics (AQTR 2010)*, Vol. 3, pp. 105-110, ISBN 978-1-4244-6724-2, Cluj-Napoca, Romania, May 2010

Hafiane, A., Zavidovique, B., and Chaudhuri, S. (2005). A modified FCM with optimal Peano scans for image segmentation, *Proceedings of the 2005 IEEE International*

*Conference on Image Processing (ICIP 2005)*, Vol. 3, pp. 840-843, ISBN 0-7803-9134-9, Genoa, Italy, September 2005

Marshall, B. D., Neymark, L.A., and Peterman, E.Z. (2003). Estimation of past seepage volumes from calcite distribution in the Topopah Spring Tuff, Yucca Mountain, Nevada. *Journal of contaminant hydrology,* Vol. 62-63 (April-May 2003), pp. 237-247, ISSN 0169-7722

Najjar, Y. M., Basheer, I.A., and Naouss, W.A. (1996). On the Identification of Compaction Characteristics by Neuronets. *Computers and Geotechnics*, Vol. 18, No. 3, pp. 167-187, ISSN 0266-352X

O'Conaire, C., O'Connor, N., Cooke, E., and Smeaton, A.F. (2006). Comparison of Fusion Methods for Thermo-Visual Surveillance Tracking, *Proceedings of the 9th International Conference on Information Fusion (FUSION 2006)*, pp. 1-7, ISBN 1-4244-0953-5, Florence, Italy, July 2006

Ohnishi, Y., and Soliman, M. (1995). Seepage Under Concrete Dam Founded on Rock Formation using Artificial Neural Networks, *Proceedings of the International Workshop on Rock Foundation of Large Scale Structures,* pp. 355-360, Tokyo, Japan, September 1995

Ollero, A., Martinez-De Dios, J.R., and Arrúe, B.C. (1998). Integrated systems for early forest-fire detection, *Proceedings of the 3rd International Conference on Forest Fire Research and 14th Conference on Fire and Forest Meteorology*, Vol. 2, pp. 1977-1988, ISBN 972-97973-0-7, Luso, Portugal, November, 1998

Platt, J. (2000). Probabilistic outputs for support vector machines and comparisons to regularized likelihood methods, In: *Advances in Large Margin Classifiers*, Smola, A., Bartlett, P., Schölkopf, B., and Schuurmans, D., pp. 61-74, MIT Press, ISBN 0262194481, Cambridge, MA

Shaomin, L., Hai, S., and Cheng, W. (2009). Flood Simulation and Information Management System's Design and Implement, *Proceedings of the 1st International Workshop on Education Technology and Computer Science (ETCS 2009)*, Vol. 1, pp.737-740, ISBN 978-1-4244-3581-4, Wuhan, Hubei, China, March 2009

Shi, S., Ye, X., Dong, Z., and Zhou, H. (2006). Research on the Integration of GIS-Based Digital Valley System, *Proceedings of the 1st International Multi-Symposiums on Computer and Computational Sciences (IMSCCS 2006*), Vol. 1, pp. 452-457, ISBN 0-7695-2581-4, Hangzhou, Zhejiang, China, June 2006

Sieh, D., King, D., and Gientke, F. (1988). Dam Seepage Analysis Using Artificial Intelligence, In: *Planning Now for Irrigation and Drainage in the 21st Century*, DeLynn, H., pp 417-422, American Society of Civil Engineers (ASCE), ISBN 9780872626669, New York, N.Y.

Vapnik, V.N. (1998). *Statistical Learning Theory* (1st Edition), Wiley-Interscience, ISBN 0471030031, New York

Wen, Z., Wu, Z., and Su, H. (2004). Safety monitoring system of dam based on bionics, *Proceedings of 2004 International Conference on Machine Learning and Cybernetics*, Vol. 2, pp. 1099 – 1104, ISBN 0-7803-8403-2, Shanghai, China, August 2004

Yin, Z., and Malcolm, A. (2000). Thermal and Visual Image Processing and Fusion, *SIMTech Technical Report AT/00/016/MVS*, Retrieved from http://www.simtech.a-star.edu.sg/Research/TechnicalReports/TR0630.pdf

Zhou, Y., and Huang, J. (2007). An AHP-Based Fuzzy Evaluation Approach to Management of Sustainable Water Resources, *Proceedings of the 2007 International Conference on Wireless Communications, Networking and Mobile Computing* (WiCom 2007), pp. 5025 – 5028, ISBN 978-1-4244-1311-9, Shanghai, China, September 2007

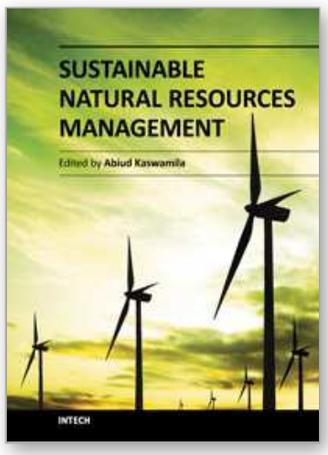


**Sustainable Natural Resources Management**
Edited by Dr. Abiud Kaswamila

ISBN 978-953-307-670-6
Hard cover, 166 pages
**Publisher** InTech
**Published online** 13, January, 2012
**Published in print edition** January, 2012

Natural resources conservation is one of the dilemmas currently facing mankind in both developed and the developing world. The topic is of particular importance for the latter, where the majority depend on terrestrial ecosystems for livelihood; more than one billion people live in abject poverty earning less than a dollar per day; more than 3.7 billion suffer from micronutrient deficiency and more than 800 million suffer from chronic hunger. Population increase, resource use conflicts, technological advancements, climate change, political doldrums, and unsustainable use and harvesting of resources have all put more pressure on natural resources leading to land degradation and poverty. To achieve a win-win situation, we need to change our mindset by thinking outside the box through advocating integrated and holistic approaches in managing our natural resources. This book presents a variety of sustainable strategies and/or approaches including use of GIS and Remote Sensing technologies, decision support system models, involvement of stakeholders in major decisions regarding use of natural resources, community level initiatives, and use of surveillance and monitoring mechanisms.

**How to reference**
In order to correctly reference this scholarly work, feel free to copy and paste the following:

Gordan Mihaela, Dancea Ovidiu, Cislariu Mihaela, Stoian Ioan and Vlaicu Aurel (2012). Fuzzy Image Processing, Analysis and Visualization Methods for Hydro-Dams and Hydro-Sites Surveillance and Monitoring, Sustainable Natural Resources Management, Dr. Abiud Kaswamila (Ed.), ISBN: 978-953-307-670-6, InTech, Available from: http://www.intechopen.com/books/sustainable-natural-resources-management/fuzzy-image-processing-analysis-and-visualization-methods-for-hydro-dams-and-hydro-sites-surveillanc

INTECH
open science | open minds

**InTech Europe**
University Campus STeP Ri
Slavka Krautzeka 83/A
51000 Rijeka, Croatia
Phone: +385 (51) 770 447
Fax: +385 (51) 686 166
www.intechopen.com

**InTech China**
Unit 405, Office Block, Hotel Equatorial Shanghai
No.65, Yan An Road (West), Shanghai, 200040, China
中国上海市延安西路65号上海国际贵都大饭店办公楼405单元
Phone: +86-21-62489820
Fax: +86-21-62489821

IntechOpen